Tuning electronic properties of the S_2/graphene heterojunction by strains from density functional theory*

Jun-Hui Lei(雷军辉), Xiu-Feng Wang(王秀峰), and Jian-Guo Lin(林建国)†

Materials Science and Engineering,Xiangtan University, Xiangtan 411105, *China*

(Received 16 July 2017; revised manuscript received 24 August 2017; published online 20 November 2017)

Based on the density functional calculations, the structural and electronic properties of the WS_2/graphene heterojunction under different strains are investigated. The calculated results show that unlike the free mono-layer WS_2, the monolayer WS_2 in the equilibrium WS_2/graphene heterojunctionis characterized by indirect band gap due to the weak van der Waals interaction. The height of the schottky barrier for the WS_2/graphene heterojunction is 0.13 eV, which is lower than the conventional metal/MoS_2 contact. Moreover, the band properties and height of schottky barrier for WS_2/graphene heterojunction can be tuned by strain. It is found that the height of the schottky barrier can be tuned to be near zero under an in-plane compressive strain, and the band gap of the WS_2 in the heterojunction is turned into a direct band gap from the indirect band gap with the increasing schottky barrier height under an in-plane tensile strain. Our calculation results may provide a potential guidance for designing and fabricating the WS_2-based field effect transistors.

Keywords: WS_2/graphene heterojunction, density functional theory (DFT), Schottky barrier, direct/indirect band gap

PACS: 71.15.Mb, 71.20.–b, 82.65.+r, 68.47.Fg **DOI:** 10.1088/1674-1056/26/12/127101

1. Introduction

Much attentionhas been paid to two-dimensional (2D) materials owing to their distinctive performances such as extraordinary electronic, optical, mechanical, chemical and thermal properties, recently.[1–5] The excellent 2D materials are expected to be an alternativeto the next-generation optoelectronic and nano-electronic devices. The first 2D material that has aroused great interest is graphene. Graphene, a carbon monolayer material hybridized by sp^2 orbits, has been widely investigated due to its remarkable properties.[2,6–8] However, the gapless nature of monolayer graphene has restricted its applications. Recently, a bland new class of 2D material, such as the transition metal dichalcogenides (TMDCs), provides a new research field.[9,10] The WS_2 is a member of the most studied TMDCs. The bulk WS_2 is a layered material with the neighboring layers held by weak van der Waals (vdW) force. Unlike gapless graphene, the bulk WS_2 is a semiconductor with an indirect band gapof 1.4 eV. However it can be tailored into a direct band gap (2.1 eV) material when exfoliated into a monolayer state. The monolayer WS_2 is sandwiched structure comprised of a tungsten layer and two sulphur layers. The monolayer WS_2, with a relatively small band gap, can be used as a barrier material in increasing the ON/OFF ratio of the field effect transistors (FETs). Excellent performances have been found in the heterostructure consisting of the layered WS_2 and graphene.[11,12] At present the heterostructures held by the vdW interaction open a hot research field. The heterostructures are vertical stacks of 2D layers of dissimilar materials. In the heterostructures held by vdW interaction, some intrinsic electronic properties of the individual materials can be preserved, at the same time some particularly advantageous properties can be created.[13–16] Experimental and theoretical investigation show that the heterostructures such as graphene/MoS_2,[13,17] graphene/hexagonal boron nitride,[18–23] graphene/silicone,[24,25] and graphene/phosphorene[16,26,27] are novel materials with wide application prospects due to their light weight, low power consumption and flexibility. The improvement of the electron transfer rate and the electrochemical performance can be achieved by the growth of WS_2 on graphene.[11] The applications of the WS_2/graphene heterojunction (WGH)is mainly restricted by its electronic properties. The direct band gap and suitable energy barrier, which are beneficial for electronic transmission and photoelectric switch, are expected. The electronic properties of the ultrathin WS_2 in the WGH are seldom discussed theoretically. In the article, we focus on tuning the electronic properties of the WGH based on the density-functional theory calculation.

Strain engineering has been identified as one of the best possible strategies to tune the energy band of single layer material.[27–31] For example, the Peelaers and Van de Walle's work[32] showed that the band gap reduction of the crystal structure of MoS_2 under uniaxial compressive strain was induced by the conduction band minimum (CBM) and valence band maximization (VBM) moving toward each other, further the direct band can turn into an indirect band by apply-

*Project supported by the National Natural Science Foundation of China (Grant No. 11202178).

†Corresponding author. E-mail: lin_j_g@xtu.edu.cn

© 2017 Chinese Physical Society and IOP Publishing Ltd

ing strain. Recently, Liu *et al.*[31] has predicted the contacted properties (n-Schotty or p-Schotty) of heterostructure can be tuned by the biaxial strain, at the same time the Schotty height can be controlled by strain. The application of strain is an effective and experimental method for band engineering of the 2D materials, which can sustain much larger strains than the bulk crystals, and practical strain experiments have shown the results consistent with theoretical predictions.[32,33] Ganatra and Zhang have pointed that the electronic properties of few layers MoS_2 can be tailored for specific application.[34] Therefore, we expect to tune the electronic properties(band type and n-Schotty barrier height) of the WGH by different strains.

In the present work, the electronic properties of the WGH are investigated by first principles calculations. The calculated results show that due to the weak vdW force between the graphene and the monolayer WS_2, the monolayer WS_2 of the equilibrium WGH is characterized by an indirect band gap, which is different from the free monolayer WS_2. The schottky barrier height of the WGH at the equilibrium structure is 0.13 eV (lower than the conventional MoS_2/metal), the low schottky barrier is beneficial to electronic transport. In addition, we will use in-plane strains to modulate the electronic properties of the WGH, and we find that the schottky barrier height (SBH) of the single layer WS_2 in the WGH can be reduced into zero when applying compressive strains. Particularly the direct band gap of the monolayer WS_2 in the WGH can be attained when applying tensile strains. Our studies may provide some instrumental guidance in designing and fabricating the nano-devices held by vdW force for FETs.

2. Computational method and model

All the work is done by Vienna *Ab-initio* Simulation Package (VASP),[35–38] based on the density-functional theory, with the projected augmented wave (PAW) method implemented. The exchange–correlation functional is described by the generalized gradient approximation (GGA) of the Perdew–Burke–Ernzerhof (PBE) functional.[39–41] A general drawback of all common GGA functions is that they cannot describe the long-range electron correlations that are responsible for vdW forces. To overcome the drawback, the van der Waals density functional 2 (vdW + DF2) proposed by Grimme,[42–44] which describes the long-range vdW interactions well, is included in our calculations. The calculations are performed with Brillouin zone (BZ) sampled by $5\times5\times1$ Monkhorst–Pack k-point mesh, and the wave function of single electron in the effective field is expanded by plane-waves with the energy cutoff at 550 eV. During the ionic relaxation, the shape and size of the super cell are fixed and the atoms are allowed to be fully relaxed. The stopping criterion for the ionic relaxation is that the Hellmann–Feynman force on each atom is below 0.01 eV/Å. For the electronic optimization, the convergence criterion of energy is set to be 10^{-4} eV.

The calculated lattice parameters of the monolayer WS_2 and graphene are 3.16 Å and 2.46 Å, respectively, which are reasonable.[11] The WGH is build by the graphene as a substrate matched with the WS_2. The unit cell of our model is composed of 2×2 unit cells of WS_2 and 3×3 unit cells of graphene along with rotating 19. For the hybrid structure, the lattice mismatch is near 3%, which can be tolerated. In order to avoid the interactions between the adjacent slabs, a vacuum space of 15 Å is added along the z direction. The diagrammatic geometric configuration of WGH is depicted in Figs. 1(a) and 1(b).

For the WS_2 layer combining with graphene layer by vdW interaction, the vertical interlayer distance (marked by d in Fig. 1(a)) is crucial to eliminate the spurious interactions. In order to obtain the right vertical interlayer distance of the WS_2 layer with respect to the graphene one, the WS_2-graphene configuration is fully relaxed, with the shape and lattice parameter fixed firstly. Then the configuration is re-optimized by different interlayer distance, with the atom position along the z direction remaining unchanged. The binding energy ΔE (eV/cell) between the layer of WS_2 and graphene one is calculated as a function of d according to

$$\Delta E = \left[E_{\mathrm{WS2/Gr}} - (E_{\mathrm{WS2}} + E_{\mathrm{Gr}})\right],$$

where $E_{\mathrm{WS2/Gr}}$, E_{WS2}, and E_{Gr} are the total energies of the WGH, the isolated monolayer WS_2 and graphene sheet, respectively. The calculated results are shown in Fig. 1(c).

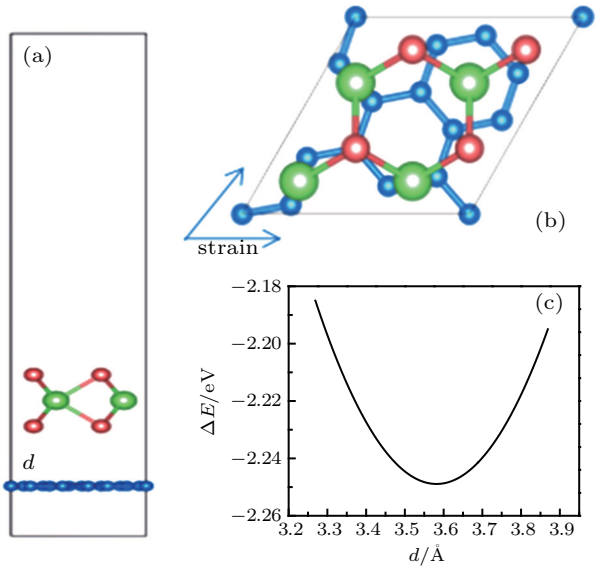


Fig. 1. (color online) Side (a) and top (b) view of the WS_2/graphene heterojunction. The C, W, and S atoms are shown as blue, green, and red balls, respectively. (c) Evolution of the total energy as a function of displacement d of the WS_2 layer relative to graphene.

3. Results and discussion

At first, the equilibrium interfacial distance is acquired by fitting the bind energy versus the interlayer distance (d) of the

WGH, and we find that the value is 3.57 Å. According to the long interfacial distance value, we can infer that the interfacial interaction should be very weak. To verify it , the reduced binding energy (E_{rb}) per carbon atom between the WS_2 monolayer and the graphene at the equilibrium vertical interlayer distance is calculated from $E_{rb} = \Delta E_{eq}/N_c$, where the ΔE_{eq} is the binding energy of the WGH at the equilibrium vertical interlayer distance and $N_c = 14$ is the number of carbon atoms in the unit cell. The calculated binding energy per C atom is -22.7 meV, which agrees well with the result of the heterostructure contacted by the vdW force.[26] According to the equilibrium interfacial distance and negligible reduced binding energy, it can be concluded that the electronic coupling in the WGH is very weak. The above results ensure the PBE functional corrected by vdW + DF2 feasibility.

Then, the electronic properties of the WGH at the equilibrium distance are studied. Figure 2(a) shows the electronic band structures of the WGH at the equilibrium interfacial distance, and the contributions from the WS_2 monolayer and graphene sheet are denoted by the blue and red line, respectively. We find that the WS_2 part in the WGH is a semiconductor with an indirect band gap of about 1.22 eV, which is different from the free WS_2 (direct band gap about 2.1 eV). This can be explained as follows. The free single-layer WS_2 is a semiconductor with the direct band gap (2.1 eV), while the bulk WS_2 held by vdW interaction is a semiconductor with an indirect-band gap of 1.4 eV. The monolayer WS_2 connected by the graphene sheet will result in the transformation from the direct band of pristine WS_2 sheet to the indirect band and the reduction of band gap. At the same time it is found that the intrinsic electronic properties of the graphene (the gapless nature and linear dispersion relationship around the Fermi level) [45] are retained.

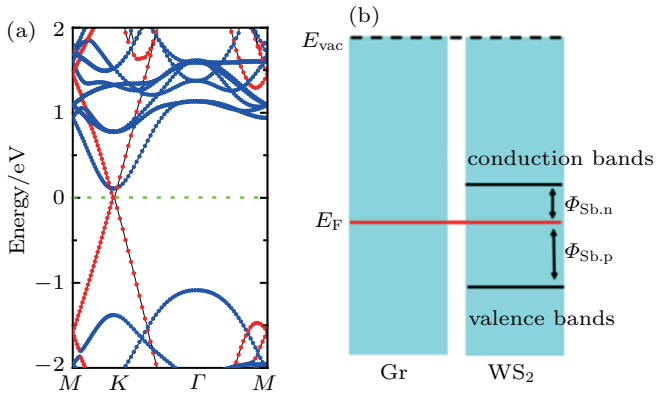


Fig. 2. (color online) (a) Electronic band structures of WS_2/graphene heterostructure at the equilibrium distance. The blue and red line denote the contributions from WS_2 monolayers and graphene, respectively. The Fermi level is set to be zero and marked by green dotted lines. (b) Schematic diagram of the Gr/WS_2 interface contact. The n-type (p-type) Schottky barrier height is the energy difference between the CBM (VBM) and the Fermi level.

The WS_2-graphene configuration is a representative of metal-semiconductor contact heterojunction. The performance of the WGH is dependent extremely on the electronic property of the WS_2 sheet. The Fermi level (FL) of the composite lies in the band gap region of WS_2, resulting in the formation of a schottky barrier at the interface, which is a crucial parameter for the contact. For the rectifying contact, the relative alignment of the semiconductor VBM or CBM to the FL of the combined system is the heterostructure intrinsic property, which is defined as schottky energy barrier. As shown in Fig. 2(b), The n-type Schottky barrier ($\Phi_{SB.n} = E_{CBM} - E_{FL}$) means that the Fermi level is located above the midgap (CBM + VBM)/2, which is an energy barrier for electronic transmission. On the contrary, the p-type Schottky barrier ($\Phi_{SB.p} = E_{FL} - E_{VBM}$) means that the Fermi level is located down the midgap, which is a barrier for hole transport. The n-type (p-type) Schottky barrier height (SBH) is the energy difference between FL and CBM (VBM). Figure 2(a) shows that the monolayer WS_2 is an n-type semiconductor with the SBH about 0.13 eV, which is lower than the conventional metal/MoS_2 contact (0.5 eV$\sim$ 1 eV).[46–51]

Due to the lattice mismatch between the parent structures, applying strain is a simple and effective method to module the electronic properties of the WGH. To show the influence of strains on the electronic properties of the WGH, the electronic properties under different in-plane biaxial strains is discussed. The in-plane biaxial strain ε (shown in Fig. 1(b)), which denotes that the strain is applied along the x direction and y direction at the same time, can be defined as follows: $\varepsilon = (a_0 - a)/a_0 = \Delta a/a_0$, where a_0 and a are the in-plane lattice constants of the unstrained and strained WGH, respectively. The ε with positive/negative value means compressive/tensile strain. The band structures of the WGH under different in-plane biaxial strains are shown in Fig. 3. The in-plane strain applied varies from -6% to 6%inlength steps of 2%. The blue and red line represent the contributions from WS_2 monolayer and graphene sheet, respectively. It is shown that the Dirac point of graphene always lies at the FL under different strains, which means that the intrinsic electronic properties of the graphene are still kept. From the energy band plots shown in Figs. 3(a)–3(c), with the strain varying from 2% to 6%, the indirect band characters of the WS_2 part in the WGH is reserved because the CBM is located at K point and VBM is located at Γ point. However as shown in Figs. 3(d)–3(f), with the strain varying from -2% to -6%, both the CBM and VBM of the monolayer WS_2 are located at K point, which indicates that the monolayer WS_2 in the WGH is characterized by a direct band gap when applying an tensile strain. Therefore, the band of the single WS_2 in the WGH can be tuned effectively by applying different strains.

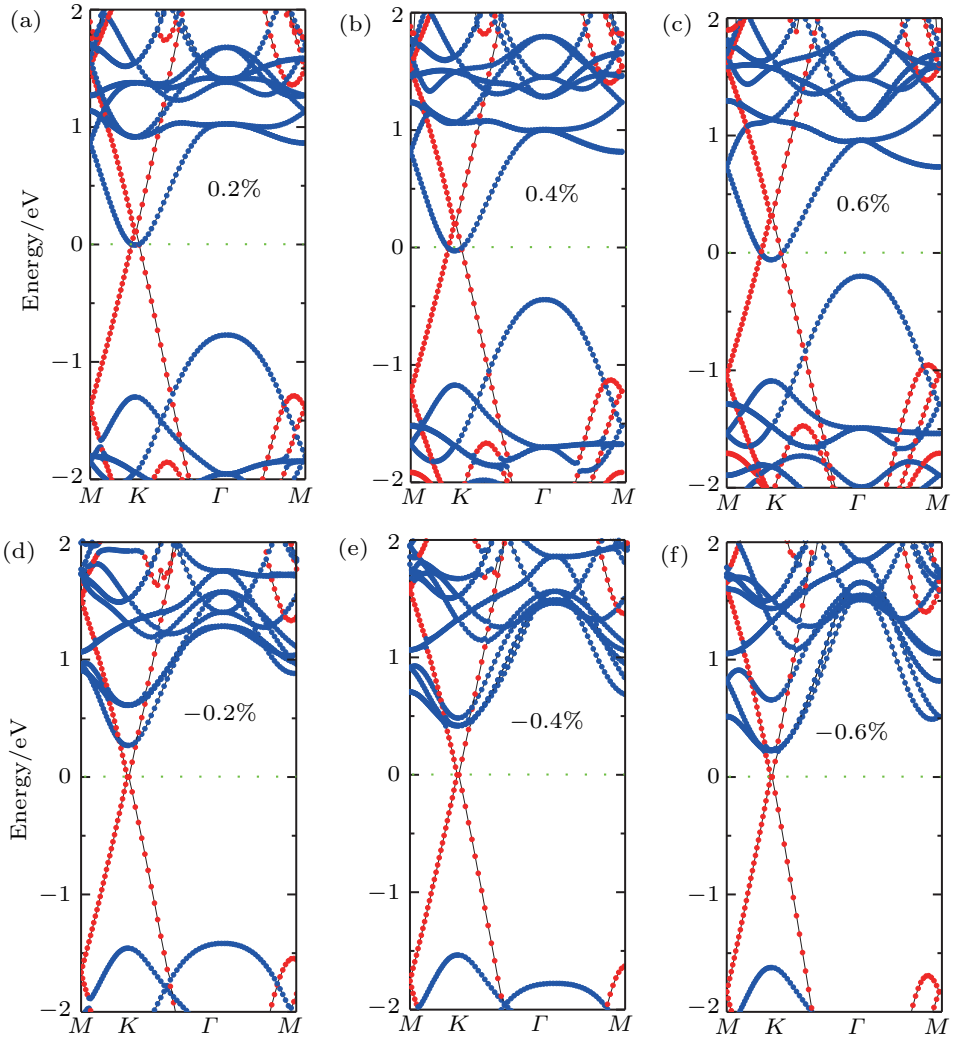


Fig. 3. (color online) Band structures of the WS_2/graphene heterostructure under different strains. Blue and red denote the contributions from WS_2 monolayers and graphene, respectively. Panels (a)–(g) show the strains of 2%, 4%, 6%, −2%, −4%, and −6%, respectively. The Fermi level is set to be zero and denoted by green dotted line.

Table 1. Calculated values of CBM (SBH), VBM, band gaps under strains from −6% to 6%. The "D" and "I" represent direct band gap and indirect band gap, respectively. To show the structural properties, the values of interlayer distance (d) under different strains are also listed here.

Stress/%	d/Å	CBM/eV	VBM/eV	gap/eV	Type
–6	3.46	0.23	–1.62	1.85	D
–4	3.46	0.42	–1.54	1.96	D
–2	3.47	0.27	–1.46	1.73	D
0	3.57	0.13	–1.09	1.22	I
2	3.61	0	–0.77	0.77	I
4	3.66	–0.03	–0.45	0.42	I
6	3.83	–0.06	–0.20	0.14	I

In order to study SBHs of the WGH under different strains, the magnitudes of CBM and VBM of the monolayer WS_2 are shown in Table 1. The results show that n-type SBHs of the WGH under the compressive strains of 2%, 4%, and 6% are 0 eV, −0.03 eV, and −0.06 eV, respectively and n-type SBHs under tensile strains of −2%, −4%, and −6% are 0.27 eV, 0.42 eV, and 0,23 eV, respectively. The change of SBHs in the WGHis induced by the FL shifting under the in-plane biaxial strain.[26,27] The compressive strains induce the FL of the WGH to move up, even to pass through the CBM, while the tensile strain causes the FL to move down, resulting in the SBHs increasing. Although the magnitude of SBHis nearly zero under compressive strain, the WS_2 part in heterostructures keeps an indirect band gap, which is the disadvantage to electronic transport. However the WS_2 part of the WGH under tensile strain keeps the direct band gap, and the SBH is still low. Hence, the tensile strain is beneficial to the enhancing of optoelectronic conversion efficiency and electronic transmission due to the direction band gap and low SBH.

In order to apperceive the conversion of electronic properties in WGH from microcosmic prospect, the charge densities of the CBM and the VBM of the WGH are shown in Figs. 4(a)–4(f). The charge densities of the CBM and the VBM under the strains of 0%, 6%, and −6% are shown in panels (a) and (d), (b) and (e), (c) and (f), respectively. The

results reveal that the electronic states near the CBM and the VBM are mainly from the contribution of W atoms. It is clear that the CBM is completely dominated by the d_{z2} orbits of W atoms under different strains. However, the VBM exhibits strong in-plane orbital characters (d_{xy} and d_{x2+y2}) with negligible contribution from the d_{z2} orbit in the WGH. Therefore, the band gap characters of the WGH are mainly determined by orbits of W atoms, which is consistent with previous theoretical study.[42] Further, a comparison among Figs. 4(a)–4(c) shows that the S atoms and W atoms present hybridization in the WGH under −6% strain, which is different from under the 0% or 6% strain. It can be inferred that the hybridization induces the formation of direct band gap.

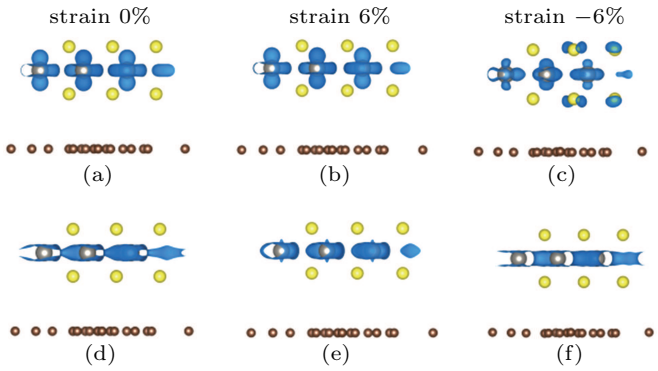


Fig. 4. (color online) Electric charge densities of CBM and VBM calculated from the WS_2/graphene heterostructure under strains of ((a) and (d)) 0%, ((b) and (e)) 6% and ((c) and (d)) −6%, respectively.

To further sustain our speculation, the local density of states (DOS)of W atoms and S atoms under the strains of 0%, 6%, and −6% in the WGH are shown in Fig. 5. In Fig. 5(a), we find that the orbital characteristics above FL are occupied by S-p_y orbits under 0% strain and the orbital characteristics below FL are occupied by S-p_z orbits. To study the integral electronic properties, we show the total DOS and local DOS of total W atoms, total S atoms and total C atoms of the balanced WGH in Fig. 5(b). We find that the orbits of W atoms, S atoms and C atoms are hardly hybrid with each other. In Fig. 5(c), we find that the orbital characteristics near FL are determined by W-d_{z2} orbits under 0% strain, which is consistent with the charge densities shown in Fig. 4(a). When exerting the strain of 6% on the WGH, the orbital characteristics are basically consistent with those of the 0% configuration as shown in Fig. 5(d). However from Fig. 5(e), we find that the orbits of W-d_{z2} and S-p_z present hybridization above fermi level, which is in accordance with the charge densities in Fig. 4(c). Further as shown in Fig. 5(f), we find that the S atoms hybridize not only with W-d_z^2, but also with W-d_x^2 and W-d_{xy}. Therefore, it can be inferred that the direct band character of the WS_2 partly kept in the WGH under the tensile strain originates from the hybridization between the S atoms orbits and the W-d_z^2, W-d_x^2, and W-d_{xy} orbits.

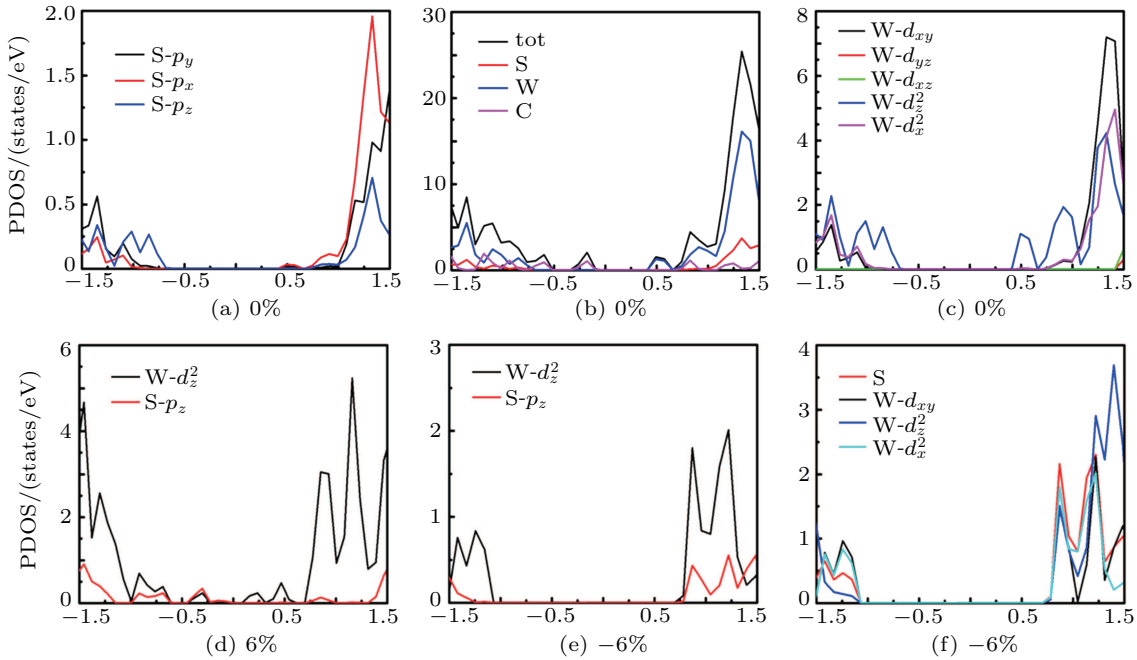


Fig. 5. (color online) Local densities of states of W atoms and S atoms under the strains of ((a)–(c)) 0%, (d) 6%, and ((e) and (f)) −6% in the WS_2-graphene heterostructure, respectively.

4. Conclusions

The structural and electronic properties of the WGH under different strains are investigated based on the density functional calculations. It is found that the monolayer WS_2 of the equilibrium WGH is characterized by indirect band gap and the electronic structure of graphene is unperturbed significantly due to the weak vdW interaction. The SBH of the equilibrium WGH is lower than the conventional metal/MoS_2 con-

tact. The indirect band gap of WS_2 is kept in the heterojunction under compressive strain. While applying in-plane tensile strains, we find that the direct band gap of the free monolayer WS_2 is recovered, which is because S atoms orbits hybridize with the W-d_z^2, W-d_x^2, and W-d_{xy} orbits from the electron structure calculation. Our calculation results show that the direct band gap and low SBH of the WGH are acquired by applying tensile strains, which is favorable for electronic transmission. This may provide an instrumental technology for fabricating the WS_2-based field effect transistors.

References

[1] FerrariA C, Meyer J C, ScardaciV, Casiraghi C, Lazzeri M, Mauri F, Piscanec S, Jiang D, Novoselov K S and Roth S 2006 *Phys. Rev.Lett.* **97** 187401

[2] Castro Neto A H, Guinea F, Peres N M R, NovoselovK S and Geim A K 2009 *Rev. Mod. Phys.* **81** 109

[3] Mak K F, Lee C, Hone J, Shan J and Heinz T F 2010 *Phys. Rev. Lett.* **105** 136805

[4] Splendiani A, Sun L, Zhang Y B, Li T S, Kim J, Chim C Y, Galli G and Wang F 2010 *Nano Lett.* **10** 1271

[5] Wu Y Q, Lin Y M, Bol A A, Jenkins K A, Xia F N, Farmer D B, Zhu Y and Avouris P 2011 *Nature* **472** 74

[6] Geim A K and Novoselov K S 2007 *Nat. Mater.* **6** 183

[7] Sprinkle M, Siegel D, Hu Y, Hicks J, Tejeda A, Taleb-Ibrahimi A, Le Fevre P, Bertran F, Vizzini S, Enriquez H, Chiang S, Soukiassian P, Berger C, de Heer W A, Lanzara A and Conrad E H 2009 *Phys. Rev. Lett.* **103** 226803

[8] Ba S H, Lee Y, Sharma B K, Lee H J, Kim J H and Ahn J H 2013 *Carbon* **51** 236

[9] Eknapakul T, King P D C, Asakawa M, Buaphet P, He R H, Mo S K, Takagi H, Shen K M, Baumberger F, Sasagawa T, Jungthawan S and Meevasana W 2014 *Nano Lett.* **14** 1312

[10] Yoon Y, Ganapathi K and Salahuddin S 2011 *Nano Lett.* **11** 3768

[11] Georgiou T, Jalil R, Belle B D, Britnell L, Gorbachev R V, Morozov S V, Kim Y J, Gholinia A, Haigh S J, Makarovsky O, Eaves L, Ponomarenko L A, Geim A K, Novoselov K S and Mishchenko A 2012 *Nat. Nanotech.* **8** 100

[12] Gong Y J, Lin J H, Wang X L, Shi G, Lei S D, Lin Z, Zou X L, Ye G L, Vajtai R, Yakobson B I, Terrones H, Terrones M, Tay B K, Lou J, Pantelides S T, Liu Z, Zhou W and Ajayan P M 2014 *Nat. Mater.* **13** 1135

[13] Liu B, Wu L J, ZhaoY Q, Wang L Z and Cai M Q 2016 *RSC Adv.* **6** 92473

[14] Liu B, Wu L J, Zhao Y Q, Wang L Z and Cai M Q 2016 *Eur. Phys. J. B* **89** 80

[15] Geim A K and Grigorieva I V 2013 *Nature* **499** 419

[16] Padilha J E, Fazzio A and da Silva A J R 2015 *Phys. Rev. Lett.* **114** 066803

[17] Zhang W J, Chu C P, Huang J K, Chen C H, Tsai M L, Chang Y H, Liang C T, Chen Y Z, Chueh Y L, He J H, Chou M Y and Li L J 2014 *Sci. Rep.* **4(7484)** 3826

[18] Su J, Feng L P, Zhang Y and Liu Z 2016 *Phys. Chem. Chem. Phys.* **18** 16882

[19] Dean C R, Young A F, Meric I, Lee C, Wang L, Sorgenfrei S, Watanabe K, Taniguchi T, Kim P, Shepard K L and Hone J 2010 *Nat. Nanotech.* **5** 722

[20] Xue J M, Sanchez Y J, Bulmash D, Jacquod P, Deshpande A, Watanabe K, Taniguchi T, Jarillo-Herrero P and Leroy B J 2011 *Nat. Mater.* **10** 282

[21] He Jun, Chen K Q, Fan Z Q, Tang L M and Hu W P 2010 *Appl. Phys. Lett.* **97** 193305

[22] Xie Z X, Zhou W X, Tang L M and Chen K Q 2016 *Carbon* **100** 492

[23] Peng J, Zhou Y H and Chen K Q 2015 *Org. Electron.* **27** 137

[24] Neek-Amal M, Sadeghi A, Berdiyorov G R and Peeters F M 2013 *Appl. Phys. Lett.* **103** 261904

[25] Cai Y, Chu C P, Wei C M and Chou M Y 2013 *Phys. Rev. B* **88** 245408

[26] Liu B, Wu L J, Zhao Y Q, Wang L Z and Cai M Q 2016 *J. Magn. Magn. Mater.* **420** 218

[27] Liu B, Wu L J, Zhao Y Q, Wang L Z and Caii M Q 2016 *Phys. Chem. Chem. Phys.* **18** 19918

[28] Ning F, Wang D, Tang L M, Zhang Y and Chen K Q 2014 *J. Appl. Phys.* **116** 094308

[29] Hui Y Y, Liu X, Jie W, Chan N Y, Hao J, Su Y T, Li L J, Guo W and Lau S P 2013 *ACS Nano* **7** 7126

[30] He K, Poole C, Mak K F and Shan J 2013 *Nano Lett.* **13** 2931

[31] Hu W, Wang T and Yang J L 2015 *J Mater. Chem. C* **3** 4756

[32] Peelaers H and Van de Walle C G 2012 *Phys. Rev. B* **86** 241401

[33] Liu B, Wu L J, Zhao Y Q, Wang L Z and Cai M Q 2015 *Phys. Chem. Chem. Phys.* **17** 27088

[34] Ganatra R and Zhang Q 2014 *ACS Nano* **8** 4074

[35] Zhao Y Q, Wu L J, Liu B, Wang L Z, He P B and Cai M Q 2016 *J. Power Sources* **313** 96

[36] Cao D, Liu B, Yu H L, Hu W Y and Cai M Q 2013 *Eur. Phys. J. B* **86** 504

[37] Cao D, Liu B, Yu H L, Hu W Y and Cai M Q 2015 *Eur. Phys. J. B* **88** 75

[38] Blochl P E 1994 *Phys. Rev. B* **50** 17953

[39] Kresse G and Furthmuller J 1996 *Phys. Rev. B* **54** 11169

[40] Grimme S and Semiempirical 2006 *Comput. Chem.* **27** 1787

[41] Zhao Y Q, Liu B, Yu Z L, Ma J M, Wan Q, He P B and Cai M Q 2017 *J. Mater. Chem. C* **5** 5356

[42] Wu L J, ZhaoY Q, Chen C W, Wang L Z, Liu B and Cai M Q 2016 *Chin. Phys. B* **25** 107202

[43] Wang L Z, ZhaoY Q, Liu B, Wu L J and Cai M Q 2016 *Phys. Chem. Chem. Phys.* **18** 22188

[44] Zhao Y Q, Liu B, Yu Z L, Cao D and Cai M Q 2017 *Electrochim. Acta* **247** 891

[45] Hu W, Wang T, Zhang R Q and Yang J L 2016 *J. Mater. Chem. C* **4** 1776

[46] Cai M Q, Du Y and Huang B Y 2011 *Appl. Phys. Lett.* **98** 102907

[47] Cai M Q, Zheng Y, Wang B and Yang G W 2009 *Appl. Phys. Lett.* **95** 232901

[48] Cao D, Cai M Q, Hu W Y, Peng J, Zheng Y and Huang H T 2011 *Appl. Phys. Lett.* **98** 031910.

[49] Cai M Q, Zheng Y and Woo C H 2011 *J. Appl. Phys.* **109** 024103.

[50] Cao D, Cai M Q and Hu W Y 2011 *J. Appl. Phys.* **109** 114107.

[51] Gong C, Colombo L, Wallace R M and Cho K 2014 *Nano Lett.* **14** 1714